

## Surface Crack Initiation and Crack Propagation of HANA-4 Cladding in an Iodine Environment

Sang Yoon Park\*, Byoung Kwon Choi, Jeong-Yong Park and Yong Hwan Jeong  
Fusion Technology Development Div., Korea Atomic Energy Research Institute,  
Daedokdaero 1045, Yuseong, Daejeon, 305-353, Korea  
\*Corresponding author: nsypark@kaeri.re.kr

### 1. Introduction

Nowadays, most nuclear power reactors are adopting a high burn-up to increase their fuel economy, where the refueling cycle of the fuel bundles is extended. As a fuel burn-up increases, the possibility of an iodine-induced stress-corrosion cracking (ISCC) is increased.

KAERI had developed six kinds of advanced Zr alloy claddings named HANA (High performance Alloy for Nuclear Application) in order to meet the global demand for an extension of the fuel discharge burn-up to more than 70 GWd/MtU. In this high burn-up condition, the diameter of the cladding is decreased but the outer diameter of the fuel pellet is increased so that the PCI behavior will be very severely. Also, the concentration of iodine inside the fuel rod increased so that the possibility of both a mechanical and a chemical interaction which causes a SCC become more severe. So the PCI resistance of HANA cladding needs to increase. This study has been done to estimate the PCI behavior of HANA-4 (Zr-1.5Nb-0.4Sn-0.2Fe-0.1Cr) cladding. The ISCC crack initiation and propagation mechanism of the HANA-4 cladding was explained well by the grain-boundary pitting coalescence (GBPC) and the pitting-assisted slip cleavage (PASC) models [1-2]. The effect of a heat treatment and the microstructure on a PCI resistance was also explained well by the GBPC and PASC models. The PCI resistance for HANA-4 was higher than that of Zircaloy-4.

### 2. Experimental

The specimens for this study were cut from a HANA-4 and Zircaloy-4 cladding. Their outer and inner diameters were 9.50 mm and 8.36 mm, respectively. Their length was 130 mm. They were all used in their as-received states namely a stress-relieved condition. To investigate the effect of the microstructure, a specimen was heat-treated at 620°C for 3 hours to have a fully recrystallized structure then it was used for the ISCC test. A specimen with an initial crack inside its surface was used in the test. A pre-crack was created by the fatigue cracking method which Lemaignan [3] employed.

Test specimen was put inside an autoclave, and then a medium, which was pure argon mixed with iodine, was pressurized inside the cladding after reaching a constant test temperature of 350°C. The iodine used in this study, which had a purification of 99.99%, was

supplied by Aldrich. The iodine concentration was kept constant at 1.5 mg/cm<sup>2</sup>. After the test, the specimen was examined using a scanning electron microscope (SEM) to determine the actual crack propagation depth during the ISCC test, and then the crack propagation velocity was calculated. ISCC crack propagation rate with respect to the applied  $K_I$  was evaluated to determine the threshold stress intensity factor ( $K_{ISCC}$ ). The  $K_I$  value was adjusted so that the stress state around a crack tip was a plane strain condition [4].

### 3. Results and Discussion

Recently, grain boundary pitting coalescence (GBPC) and pitting-assisted slip cleavage (PASC) models have been proposed to explain the ISCC crack initiation and propagation mechanism of a Zircaloy-4 surface. Fig.1 shows the inner surface crack nucleation by the GBPC model in an iodine environment for 6.9 hours under a hoop stress of 310 MPa. Numerous pits of various sizes can be seen over the entire surface. Small pits of less than 2.5  $\mu\text{m}$  tend to agglomerate with each other to form a large pitting cluster that orients along the axial direction.

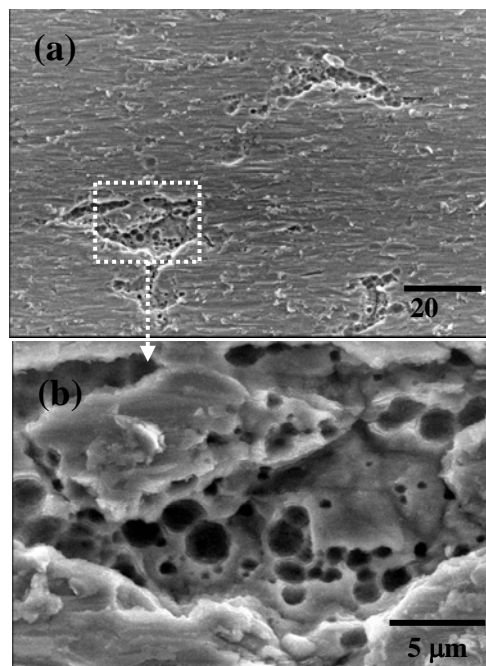


Fig. 2. Pitting morphology on the internal surface of the Zircaloy-4 cladding after an internal pressurization test,

showing a pitting agglomeration and nucleation of a crack; (a) 1000X, (b)5000X.

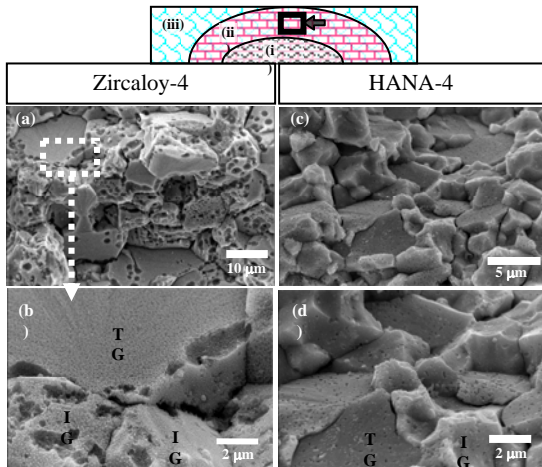


Fig. 2. Fractographs of an ISCC crack for the RX Zircaloy-4 and the RX HANA-4 cladding pressurized in an iodine environment at 350°C; (a), (b) Zircaloy-4, (c), (d) HANA-4 cladding.

Fig. 2 shows the fractographs of the recrystallized Zircaloy-4 and HANA-4 claddings for the ISCC crack surface. It was pressurized in the iodine environment at 145 MPa for 12.3 h in the case of the Zircaloy-4 cladding and at 177 MPa for 100 h in the case of the HANA-4 cladding. For the Zircaloy-4, both IG and TG cracks were observed at the same time, showing that a lot of pits and pitting clusters were developed on the IG surfaces. The size of the pits was less than 2  $\mu\text{m}$ . Regarding the TG surfaces, however, no pits were shown. The figure also shows that the majority of the GBs are severely attacked by a pitting. For the HANA-4 cladding, both IG and TG cracks were observed at the same time. In this case, the pits were fine and shallow and could be seen on the whole surface. Contrary to the result of Zircaloy-4, the GB of the HANA-4 cladding is not attacked by a pitting corrosion. It means that the pitting resistance of HANA-4 is so high that the GBPC and PASC phenomena of the HANA-4 cladding are suppressed. Therefore the increase of the pitting resistance at the GB of the HANA-4 cladding plays an important role in reducing the crack propagation rate.

Fig.3 shows the crack propagation rate of the as-received Zircaloy-4 and HANA-4 claddings with respect to the applied  $K_I$  value. We obtained a  $K_{ISCC}$  value of 3.3  $\text{MPa}\cdot\text{m}^{0.5}$  for the Zircaloy-4 and 4.5  $\text{MPa}\cdot\text{m}^{0.5}$  for the HANA-4 cladding, which means that the HANA-4 cladding has a higher resistance to a crack growth than the Zircaloy-4. The crack propagation rate in region II of the Zircaloy-4 is more than ten times greater than that of the HANA-4 cladding.

The increase of the ISCC resistance for HANA -4 cladding result from adding of Nb element in the Zr-alloy. Many pitting clusters appear on the IG surface of the Zircaloy-4, but small and shallow pits appear on the IG surface of the HANA claddings. Some pitting

clusters appear on the border of the TG surface in Zircaloy-4, but no pitting appears in the HANA claddings. Thus, the addition of Nb to Zr-alloy seems to suppress the pitting generation around the grain boundary and increase the ISCC resistance.

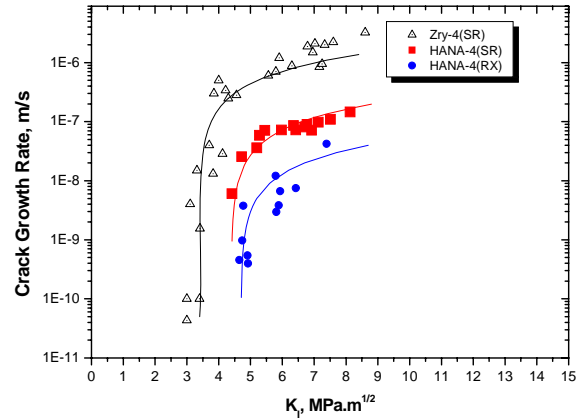


Fig. 3. Plots of  $da/dt$  vs.  $K_I$  plots for the Zircaloy-4 and HANA-4 cladding.

### 3. Conclusions

The pitting corrosion on the grain boundary is the major factor for the surface crack initiation and crack propagation of a nuclear fuel cladding. The ISCC resistance of HANA-4 cladding is higher than that of Zircaloy-4 in all the conditions. Especially, the crack propagation rate of the recrystallized HANA-4 cladding is 100 times lower than that of Zircaloy-4. The increase of the pitting resistance at the grain boundary plays an important role in reducing the crack propagation rate of HANA-4 claddings. It means that the GBPC and PASC phenomena are suppressed in HANA-4 cladding by the increasing of pitting resistance in the grain boundary.

### REFERENCES

- [1] S.Y.Park, J.H.Kim, M.H.Lee Y.H.Jeong, J. Nucl. Mater. 372 (2008) 293
- [2] S.Y. Park, J.H. Kim, B.K.Choi, Y.H. Jeong, Met. Mater. -Int, 13 (2007) 155
- [3] C. Lemaignan, Int. J. Pres. Ves. & Piping, 15 (1984) 241
- [4] Yu. K. Bibilashvily, Yu. N. Dolgov, B. I. Nesterov, V. V. Novikov, J. Nucl, Mater., 224 (1995) 307